Solvothermal Synthesis of NiS 3D Nanostructures

Wanqun Zhang,[a] Liqiang Xu,[a] Kaibin Tang,[a] Fanqing Li,[a] and Yitai Qian*[a,b]

Keywords: Nickel sulfide / Nanostructures / Complexes / Crystal growth

Highly uniform urchin-like nanostructures (in the structures, nanoneedles or nanobelts grow radially from the core particles) of NiS (millerite) were successfully prepared by a solvothermal synthetic route using $Ni(Ac)_2{\cdot}6H_2O$ and dithizone as reagents and ethylenediamine as solvent in the temperature range of 220–240 °C. The prepared nickel sulfides with urchin-like 3D architectures were characterized by X-ray diffraction (XRD), field emission scanning electron microscopy (FE-SEM) and high-resolution transmission electron microscopy (HRTEM). The reaction temperature, sulfur sources, and solvent are of great importance on the final urchin-like structures. On the basis of the experimental results, a possible growth mechanism of the urchin-like NiS crystals is proposed, which is supported by the technical characterizations.

Introduction

Many properties of crystalline materials depend on the crystallographic direction, for example, the spontaneous polarization in ferroelectrics and the magnetic coercivity and remanence in ferromagnets.[1] Over the past few years, there has been growing interest in low dimensional nanostructure semiconductors because of their novel electrical and optical properties, and potential applications in nanodevices.[2] Recently, research is expanding into the assembly of nanoparticles in two-dimensional and three-dimensional ordered superstructures.[3] Much effort has been made to construct patterns of well-arranged nanocrystallites, especially arrangements of nanotubes and nanorods due to their interesting physical properties and potential applications in many areas.[4] To obtain highly oriented growth of nanorods, solid templates are usually required, such as porous alumina, polymer nanotubes, and patterned catalysts, to control the directional growth.[5] However, the introduction of templates and substrates introduces heterogeneous impurities, increases the production cost, and thus leads to the difficulty for scale-up production. The development of facile, mild, easily controlled, and template-free methods to create novel patterns on self-generated homogeneous substrates therefore is of great significance.

Nickel monosulfide (NiS) has been the subject of considerable interest because of its properties as a metal insulator, paramagnetic–antiferromagnetic phase-changing material, and its use in hydrosulfurization catalysts and solar storage.[6] In this paper, we present the synthesis of highly uniform urchin-like 3D nickel sulfide nanostructures by the reaction between nickel acetate and dithizone (H_2DZ, $C_{13}H_{12}N_4S$) in ethylenediamine without the use of any template, polymer, and surfactant. Although Xie's group synthesized 3D NiS with flowerlike architectures via a polymer assistant, recently NiS (millerite) nanorods and triangular nanoprisms were synthesized, and other several geometrical urchin-like patterns have also been presented.[7] Up to now, there has not been a report on these kind of urchin-like 3D nickel sulfides nanostructures (in the structures, nanoneedles or nanobelts grow radially from the core particles) synthesized by a simple, efficient method under mild conditions. As a catalyst, the urchin-like nanostructures, which have highly specific area on the surface of the particles, may provide directional catalyst ability and realize region-dependent surface reactivity.

Results and Discussion

Figure 1 shows the XRD patterns of NiS obtained at 220 °C for 5 h. All the peaks in Figure 1 can be indexed as pure millerite NiS (space group: *R*3*m*) with cell parameters a = 9.63 Å, c = 3.15 Å, which are close to the literature data (JCPDS file number: 12–0041). Similar XRD patterns were obtained from other products of the comparison experiment, all of which exhibited millerite NiS.

The morphology of the product was determined by FR-SEM and TEM. Figure 2 shows the obtained urchin-like nanostructures synthesized at 220 °C for 5 h. After careful observation (Figure 2, b, c), it has been found that the ur-

[a] Department of Chemistry, University Science and Technology of China,
Hefei, Anhui, 230026, People's Republic of China
Fax: (internat.) +86-5513607402
E-mail: ytqian@ustc.edu.cn
[b] Structure Research Laboratory, University Science and Technology of China,
Hefei, Anhui, 230026, People's Republic of China

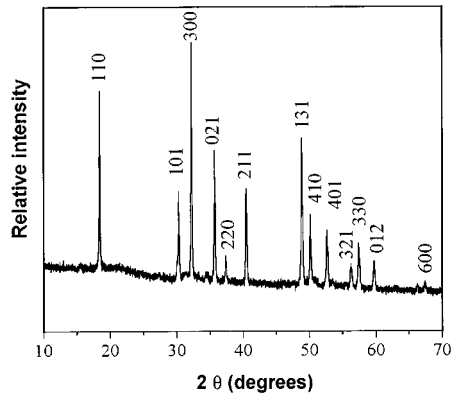

Figure 1. XRD pattern of the synthetic millerite NiS at 220 °C for 5 h

chin-like pattern usually has a diameter of about 30 μm with acicular crystallites radiating from the center in a uniform size distribution. The nanoneedles grown from the center have almost uniform diameters: the bottom of the nanoneedles is about 150 nm; the tip of the nanoneedles is about 50 nm. The nanoneedles were investigated in more detail by high-resolution transmission electron microscopy (HRTEM) (Figure 2, d) and by the SAED pattern (inset in Figure 2, d). The HRTEM image of an individual nanoneedle in Figure 2 (d) shows that lattice spacing of about 0.48 nm and 0.29 nm correspond to the (110) and (011) planes, respectively, of rhombohedral phase NiS. The obtained ED spots projected along the [1 $\bar{1}$ 1] zone axis could be indexed as millerite NiS (110) and (011) planes. The HRTEM and SAED images indicate that the nanoneedles are single crystals grown in the direction parallel to the (110) lattice planes. With a raised temperature of 240 °C, we obtained nanobelts with high aspect ratios, grown radially from the core particles. As shown in Figure 3 (a), these nanobelts have widths ranging from 20 nm to 70 nm and lengths of up to 12 μm. We have characterized these NiS nanobelts by HRTEM and SAED (Figure 3, b). The nanobelts exhibit lattice planes with a spacing of 0.48 nm parallel to the long axis of the nanobelt, which corresponds to the *d* spacing of the (110) planes of NiS (millerite). HRTEM images reveal that the nanobelts grow along the direction parallel to the (110) planes of NiS, which is similar to the nanoneedles. The inset image in Figure 3 (b) shows a typical SAED of the millerite NiS nanobelt, which was obtained by focusing the electron beam along the [0 $\bar{2}$ 1] zone axis of this nanobelt. The SAED pattern further confirms that this nanobelt is a single crystal of millerite NiS.

It is well known that H_2DZ is a good linker ligand, which can form $Ni(HDz)_2$ with Ni^{2+} under alkaline conditions.[8] The reaction in the present system is based on the formation of Ni-dithizone complexes followed by thermal decomposition of these complexes to obtain the final product. The whole reaction process may be expressed as follows:

$$Ni^{2+} + C_{13}H_{12}N_4S \rightarrow Ni(C_{13}H_{11}N_4S)_2 \rightarrow NiS$$

Different sulfur reagents were tested to reveal the dithizone effect, and the results showed that the dithizone was the optimum. When Na_2S was used, the product is a mixture of bulky particles of NiS and Ni_3S_2. When using thio-

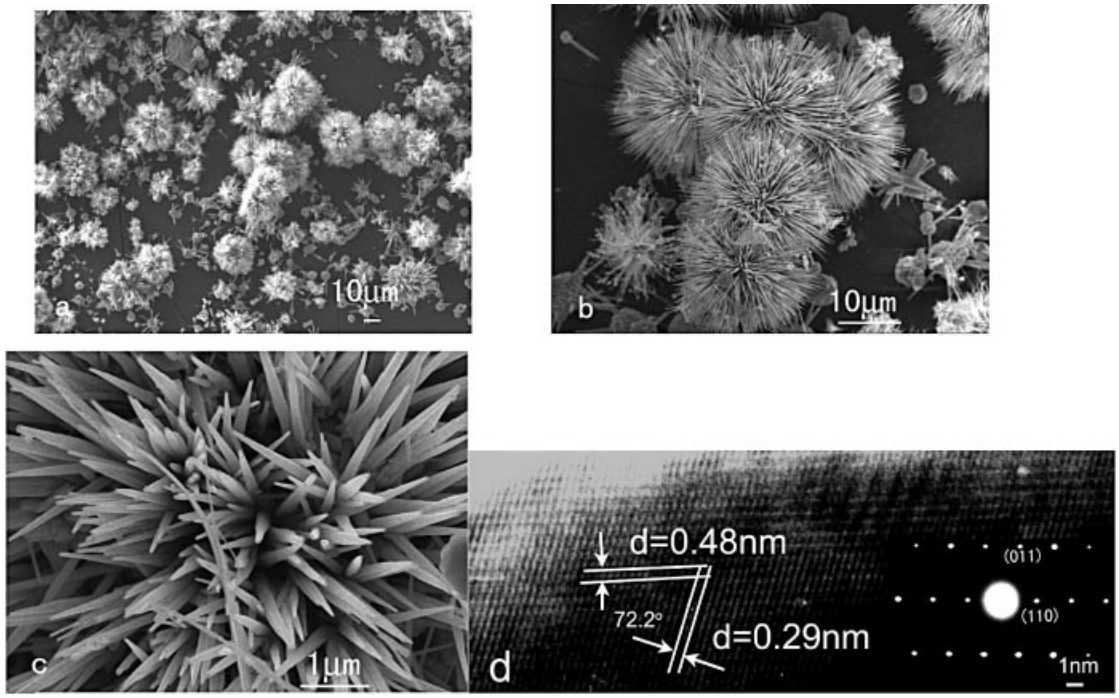

Figure 2. FE-SEM images of the synthesized urchin-like nanostructure at 220 °C for 5 h: (a) the panoramic morphologies; (b) low magnification image; (c) high magnification image; (d) HRTEM image of the NiS nanoneedles covered on urchin-like nanostructures (inset shows its corresponding ED pattern)

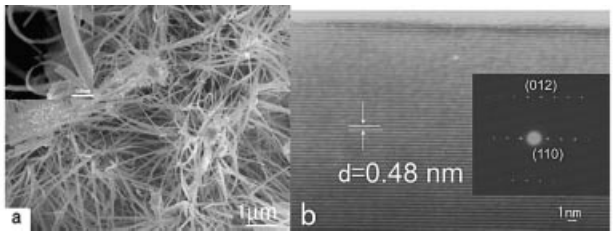

Figure 3. (a) FE-SEM image of the urchin-like nanostructure radiated with high aspect ratio nanobelts at 240 °C for 5 h, (inset shows a high-magnification FE-SEM image); (b) HRTEM image of the NiS nanobelts covered on urchin-like nanostructures (inset shows its corresponding ED pattern)

urea, podgy rods of NiS (millerite) were obtained. It is ordinarily accepted that dithizone metal complexes prevent the production of large free metal ions and sulfur ions, and thus are favorable for the oriented growth of the final product.

Generally, the growth process of crystals can be separated into two steps: an initial nucleating stage and a subsequent crystal growth process. At the initial nucleating stage, the crystalline phase of the seeds is critical for directing the intrinsic shapes of the crystals due to its characteristic symmetry and structure. In the subsequent step, the crystal growth stage is a kinetically and thermodynamically controlled process that can yield 1D and other more complicated shapes with some degree of shape tenability through changes in the reaction parameters such as temperature, reaction time, concentration, and so on.[9] In the present system, we find that the reaction temperature is undoubtedly vital in the formation of the unique urchin-like patterns of NiS nanoneedles and nanobelts. To investigate the influence of reaction temperature, the reactions were carried out at different temperatures, and the results are listed in Table 1. It is generally believed that temperature can affect crystal growth in several ways, all of them resulting in a smaller crystal size at lower temperatures. From our experiments, it can be clearly seen that a higher temperature is preferable for the anisotropic growth of crystal and results in the product with high aspect ratios (Figure 3, a). Meanwhile, at lower temperatures of 160 °C and 180 °C, only podgy rods and nail-like crystals with lower aspect ratios are obtained. Based on FE-SEM studies, by changing the reaction time a possible formation mechanism of 3D urchin-like NiS nanostructure can be obtained and is described as follows: at the beginning of the reaction, some nuclei are formed. These nuclei rapidly develope into aggregated particles (Figure 4, a). ED patterns of the aggregated particles confirm that the aggregated particles are polycrystal. All the diffraction rings in the ED patterns can be indexed to millerite NiS (inset in Figure 4, a). Because the initial growth may be too rapid to be separated from the nucleation,[10] sheets are formed on the surface of the aggregated particles (Figure 4, b), and then at elevated temperature and pressure, the layer structures directly collapse into nanorods (Figure 4, c).[11] During the following solvothermal process, the shorter nanorods may redissolve into the solution phase, and the longer nanorods grow much longer (Figure 4, d), which is similar to the formation process of silver nanowires.[12] With the rapid growth of nanorods, the concentration of the reactants decreases, which does not completely satisfy the growth of nanorods and finally results in the formation of needlelike nanocrystals (Figure 2, a). Further studies are necessary to understand the exact formation mechanism of 3D NiS nanocrystals.

Ethylenediamine also played an important role in the formation of urchin-like NiS. When Ethylenediamine was substituted by ammonia, ethylamine (65−70%), or 1,6-hexanediamine, the results, shown in Table 2, indicated that neither NiS (millerite) nor urchin-like morphology was obtained. Therefore, it is believed that the solvent affected the phase formation in the reaction system. The exact influence of the solvent undoubtedly needs further investigation.

Table 1. The relationship between temperature and different morphology products

Temperature	Time	Phase	Morphology	Figures	Aspect ratio
160 °C	5 h	–	–	–	–
160 °C	96 h	NiS	podgy rod	–	low
180 °C	5 h	NiS	nail-like	–	lower
220 °C	5 h	NiS	urchin-like (nanoneedles)	2, a	high
240 °C	5 h	NiS	urchin-like (nanobelts)	3, a	higher

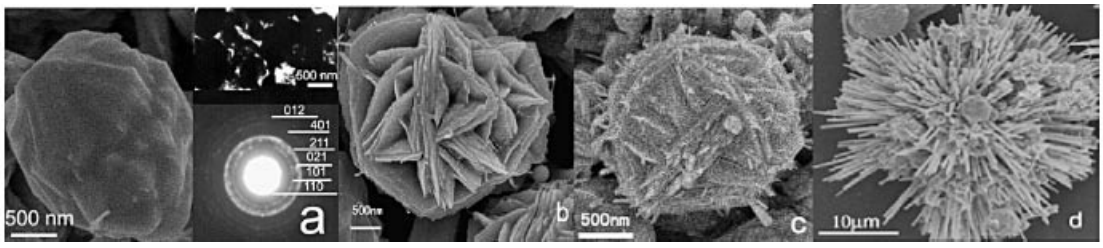

Figure 4. FE-SEM images of the products obtained by the solvothermal treatment at 220 °C for various times: (a) 30 min, the insets show the corresponding TEM and ED patterns; (b) 60 min; (c) 90 min; (d) 120 min

Table 2. Results of the reaction of $Ni(AC)_2 \cdot 6H_2O$ and dithizone at 220 °C for 5h

Solvent	Product	Morphology
ammonia/water	Ni_3S_2	irregular
ethylamine (65−70%)	Ni_3S_2, Ni_7S_6	−
1,6-hexanediamine	Ni_3S_2	spherical

Conclusion

In summary, in this paper we have developed a facile solvothermal method for the preparation of highly uniform urchin-like 3D nickel sulfide nanostructures by altering the reaction temperature. A possible mechanism was proposed to explain their formation. This low-temperature synthetic route, free of templates, polymer and surfactant, can be easily adjusted to prepare urchin-like 3D nickel sulfides and might be expanded to the preparation of other low-dimension nanomaterials.

Experimental Section

Preparation of Uniform Urchinlike Nanostructures: All the reagents were analytical grade and purchased from Shanghai Chemical. In a typical synthesis, equivalent molar amounts of $Ni(Ac)_2 \cdot 6H_2O$ and H_2DZ (1.2 mmol) were placed in ethylenediamine (50 mL), and the mixture was stirred strongly for about 1 hour to form a homogeneous solution. The resulting solution was transferred into a 60 mL Teflon-lined autoclave, which was sealed and maintained between 220−240 °C for 5 h, before being left to cool to room temperature naturally. The precipitate was filtered off, and washed with distilled water and absolute ethanol several times, and dried in vacuo at 60 °C for 4 h.

Sample Characterization: SEM images were obtained on a Hitachi (X-650) scanning electron microanalyzer and a JSM-6700F field emission scanning electron microscope (FE-SEM). XRD patterns of the products were recorded by employing a Philips X'pert X-ray diffractometer with Cu-K_α radiation (λ = 1.54187 Å). The electron diffraction (ED) patterns and high-resolution transmission electron microscopy (HRTEM) images were carried out on a JEOL-2010 TEM at an acceleration voltage of 200 kV.

Acknowledgments

Financial support from the National Science Foundation of China is gratefully acknowledged.

[1] [1a] S. J. Park, S. Kim, S. Lee, Z. G. Khim, K. Char, T. Hyeon, *J. Am. Chem. Soc.* **2000**, *122*, 8581−8582. [1b] T. Sasaki, A. Katxuragi, O. Mochizuki, Y. Nakazawa, *J. Phys. Chem. B* **2003**, *107*, 7659−7665. [1c] D. L. Leslie-Pelecky, R. D. Rieke, *Chem. Mater.* **1996**, *8*, 1770−1783. [1d] Y. W. Jun, Y. Y. Jung, J. Cheon, *J. Am. Chem. Soc.* **2002**, *124*, 615−619. [1e] N. Cordente, M. Respaud, F. Senocq, M. J. Casanove, C. Amiens, B. Chaudret, *Nano Lett.* **2001**, *1*, 565−568.

[2] [2a] Y. Cui, Q. Wei, H. Park, C. M. Lieber, *Science* **2001**, *293*, 1289−1292. [2b] G. Schmid, *Chem. Rew* **1992**, *92*, 1709−1727.

[3] [3a] R. Maoz, E. Frydman, S. R. Cohen, J. Sagiv, *Adv. Mater.* **2000**, *12*, 424−429. [3b] T. Yonezawa, S. Onous, N. Kimizuka, *Adv. Mater.* **2001**, *13*, 140−142. [3c] Z. Y. Pan, X. J. Liu, S. Y. Zhang, G. J. Shen, L. G. Zhang, Z. H. Lu, J. Z. Liu, *J. Phys. Chem. B* **1997**, *101*, 9703−9709.

[4] [4a] H Yu, P. C. Gibbons, K. F. Kelton, W. E. Bubro, *J. Am. Chem. Soc.* **2001**, *123*, 9198−9199. [4b] A. P. Alivisatos, *Science* **1996**, *271*, 933−937. [4c] A. M. Morales, C. M. Lieber, *Science* **1998**, *279*, 208−211. [4d] S. Saito, *Science* **1997**, *278*, 77−78.

[5] [5a] D. Routkevitch, T. Bigioni, M. Moskovits, J. M. Xu, *J. Phys. Chem.* **1996**, *100*, 14037−14047. [5b] H. Cao, Z. Xu, H. Sang, D. Sheng, C. Tie, *Adv. Mater.* **2001**, *13*, 121−123. [5c] M. H. Huang, S. Mao, H. Feich, H. Yan, Y. Wu, H. Kind, E. Weber, R. Russo, P. Yang, *Science* **2001**, *292*, 1897−1899.

[6] [6a] E. Wong, C. W. Sheeleigh, S. B. Rananvare, *Proceedings of the Sixth Annual Conference on Fossil Energy Materials* **1992**, 143−144. [6b] A. M Fernandez, M. T. S. Nair, P. K. Nair, *Mater. Manuf. Processes* **1993**, *8*, 535−537.

[7] [7a] F. Xu, Y. Xie, X. Zhang, C. Z. Wu, X. Wang, H. Jie, X. B. Tian, *New J. Chem.* **2003**, *27*, 1331−1335. [7b] S. Sharma, M. K. Sunkara, *J. Am. Chem. Soc.* **2002**, *124*, 12288−12293. [7c] P. Boudjouk, M. P. Remington, J. D. G. Grier, B. R. Jarabek, G. J. Mecarthy, *Inorg. Chem.* **1998**, *37*, 3538−3541. [7d] G. Z. Shen, D. Chen, K. B. Tang, F. Q. Li, Y. T. Qian, *Chem. Phys. Lett.* **2003**, *370*, 334−337. [7e] A. Ghezelbash, M. B. Sigman, Jr., B. A. Korgel, *Nano Lett.* **2004**, *4*, 537−542.

[8] [8a] G. Iwantscheff, *Das Dithizon und seine Anwendung in der Mikro-und Spurenanalyse*, 2nd ed., Verlag Chemie, Weinheim, **1972**. [8b] E. B. Sandell, *Colorimetric Determination of Trances of Metals*, Science Publishers, Inc., New York, **1959**. [8c]Freiser, *Chemist-Analyst* **1961**, *50*, 62−65. [8d] L. S. Merlwether, E. C. Breitner, C. L. Sloan, *J. Am. Chem. Soc.* **1965**, *20*, 4448−4454.

[9] [9a] Y. W. Jun, S. M. Lee, N. J. Kang, J. Cheon, *J. Am. Chem. Soc.* **2001**, *123*, 5150−5151. [9b] Y. H. Kim, Y. W. Jun, B. H. Jun, S. M. Lee, J. Cheon, *J. Am. Chem. Soc.* **2002**, *124*, 13656−13657. [9c] V. F. Puntes, D. Zanchet, C. K. Erdonmez, A. P. Alivisatos, *J. Am. Chem. Soc.* **2002**, *124*, 12874−12880. [9d] V. F. Puntes, K. M. Krishnan, A. P. Alivisatos, *Science* **2002**, *291*, 2115−2117.

[10] R. He, X. F. Qian, J. Yin, Z. K. Zhu, *J. Crystal Growth* **2003**, *252*, 505−510.

[11] X. Wang, Y. Li, *Chem. Eur. J.* **2003**, *9*, 300−306.

[12] [12a] Y. Sun, Y. Xia, *Adv. Mater.* **2002**, *14*, 833−837. [12b] Y. Sun, B. Gates, B. Mayers, Y. Xia, *Nano. Lett.* **2002**, *2*, 165−168.

Received July 19, 2004
Published Online January 7, 2005

